

## THE SEMI-ANNUAL THERMOSPHERIC DENSITY VARIATION BETWEEN 200–560 KM

L. Sehnal<sup>1)</sup>, M. Vykutilová<sup>2)</sup>, E. Illés<sup>3)</sup>, A. Horváth<sup>3)</sup>, Y. E. Helali<sup>4)</sup>, M. Y. Tawadrous<sup>4)</sup>1) *Astronomical Institute, Czechoslovak Academy of Sciences, 251 65 Ondřejov, Czechoslovakia*2) *Astronomical Observatory, 757 01 Valašské Meziříčí, Czechoslovakia*3) *Konkoly Observatory, Budapest, Hungary*4) *Helwan Observatory, Egypt*

Received 4 August 1987

## ПОЛУГОДОВАЯ ВАРИАЦИЯ ПЛОТНОСТИ ТЕРМОСФЕРЫ МЕЖДУ 200 И 500 КМ

Для выявления полугодовой вариации общей плотности термосферы использовался анализ Фурье; вариация характеризуется т. наз. „индексом плотности  $D$ “. Индивидуальные результаты отдельных лет и высот были подвержены статистическому анализу и найдена математическая формула для полугодовой вариации. Формула сравнивается с соотношением использованным в модели CIRA 72.

Fourier analysis is used to find the semi-annual variation of the thermospheric total density; the variation is characterized by the “Density index  $D$ ”. The results of the individual annual runs were subjected to statistical treatment and a formula for the semi-annual variation was found. It is then compared to the formula used in the CIRA 72 model.

**Key words:** thermosphere: density variation

## 1. Introduction

The following analysis of the semi-annual changes of the upper atmosphere density was conducted to determine the variations of the amplitudes and position of the extrema with height. After a separate determination of the variations with respect to a specific satellite and year, the statistical treatment is used to estimate the formula describing the behaviour of the semi-annual average variation.

## 2. Method of Analysis

We used the same method as in a previous paper (Sehnal et al. 1986) consisting of a regression of the observed data by a Fourier series of the second order. The data are not the raw density values but the s.c. “Density indices”,  $D$ , which were introduced by Walker (1977) to characterize just the pure semi-annual density variations. It is a ratio of the raw density to that cleared of all effects except the annual ones. Since a ratio is involved we analysed its logarithmic values. Thus, we fitted the logarithms of the density index with the function

$$(1) \quad \sum_{i=0}^n A_i \sin(i 2\pi/Pd) + \sum_{i=0}^n B_i \cos(i 2\pi/Pd),$$

where  $P = 365$  (days),  $n = 2$  and  $d$  is the day count in a year. The coefficients  $A_i$  and  $B_i$  are then obtained by the method of least-squares and lead to the final form of the semi-annual variation:

$$(2) \quad \sum_{i=0}^n C_i \sin[i 2\pi/P(d + \varphi_i)],$$

up to  $n = 2$ . We also tried to determine whether the amplitudes  $C_i$  and/or phases  $\varphi_i$  showed any changes with height. This was done again by a polynomial regression either of the amplitudes or dates of the extrema. By amplitude of the extrema we understand the ratio of the principal (October) maximum to the principal (June–July) minimum of the density index during the same year.

## 3. Data Reduction

About 14 000 density values have been determined on the basis of the observed drag of 22 satellites between 1965 and 1976. Decay rates were partly determined by the PERLO program (Horváth and Illés-Almár 1970), and partly taken from the publications of ephemeris centres. The time resolution changed from 1–2 days to about 5–10 days. All time intervals were omitted if at least 10 days time resolution could not be guaranteed. First, a “quasi-free-hand curve” was fitted by computer to the observed mean daily

Table 1

| $h$ (km) | Satellite | $A_1$   | $\varphi_1$ | $A_2$   | $\varphi_2$ | Year |
|----------|-----------|---------|-------------|---------|-------------|------|
| 208      | 1962 58 A | 0.09048 | 69.1        | 0.08708 | 113.8       | 1966 |
| 243      | 1963 09 A | 0.02755 | 37.7        | 0.07869 | 118.4       | 1966 |
| 271      | 1966 44 A | 0.03716 | 36.3        | 0.06030 | 118.4       | 1967 |
| 274      | 1966 44 A | 0.07902 | 87.0        | 0.07192 | 121.1       | 1968 |
| 276      | 1966 44 A | 0.03802 | 119.9       | 0.04512 | 123.2       | 1969 |
| 297      | 1966 44 A | 0.02763 | 131.9       | 0.06920 | 114.0       | 1970 |
| 318      | 1958 01 A | 0.03185 | 89.4        | 0.07213 | 133.6       | 1969 |
| 331      | 1958 01 A | 0.06619 | 78.9        | 0.10944 | 120.1       | 1968 |
| 338      | 1963 43 A | 0.11588 | 81.6        | 0.10564 | 115.8       | 1976 |
| 338      | 1963 43 A | 0.09570 | 75.9        | 0.06006 | 120.0       | 1975 |
| 340      | 1958 01 A | 0.06877 | 81.2        | 0.10761 | 129.6       | 1967 |
| 340      | 1963 43 A | 0.04103 | 67.7        | 0.06706 | 124.9       | 1974 |
| 342      | 1963 43 A | 0.10458 | 72.3        | 0.09184 | 117.8       | 1971 |
| 343      | 1958 01 A | 0.02358 | 42.7        | 0.07022 | 102.3       | 1966 |
| 343      | 1963 43 A | 0.06213 | 95.9        | 0.08611 | 109.6       | 1970 |
| 346      | 1960 03 B | 0.01733 | 110.6       | 0.13154 | 124.5       | 1966 |
| 346      | 1963 43 A | 0.04071 | 33.1        | 0.11064 | 116.9       | 1967 |
| 360      | 1962 15 B | 0.04624 | 140.0       | 0.09191 | 113.7       | 1970 |
| 379      | 1962 15 B | 0.04127 | 111.8       | 0.06243 | 181.8       | 1969 |
| 387      | 1962 15 B | 0.07170 | 68.9        | 0.10786 | 109.6       | 1968 |
| 393      | 1962 15 B | 0.06179 | 83.2        | 0.18230 | 124.9       | 1967 |
| 421      | 1960 14 A | 0.10937 | 76.3        | 0.10817 | 149.4       | 1975 |
| 421      | 1960 14 A | 0.11340 | 93.0        | 0.09471 | 125.8       | 1974 |
| 423      | 1960 14 A | 0.04650 | 106.3       | 0.06939 | 117.5       | 1970 |
| 423      | 1960 14 A | 0.05492 | 78.9        | 0.08231 | 98.9        | 1966 |
| 424      | 1960 14 A | 0.08221 | 79.5        | 0.11424 | 123.6       | 1968 |
| 560      | 1959 01 A | 0.17372 | 51.3        | 0.13864 | 117.8       | 1969 |

motion of the satellites,  $n(t)$ . The density values were calculated by means of the changes in  $n$ , using the theory developed by King-Hele (1964). The corresponding model values were derived from the CIRA 72 model for the real position and time of the actual drag date. The scale height values were derived from the CIRA 72 model by iteration. In calculating the indices  $D$ , each effect was taken into consideration except the semi-annual variation.  $D$ -values were determined for each day, and a running mean of 11  $D$ -values was then calculated for every two days to smooth out the short term fluctuations.

The basic data on satellites, heights and years in question are summarized in Tab. 1.

#### 4. Results

Some examples of the individual yearly variations are shown in Figs. 1 to 4. We see that the fitting of a curve just by hand would in some cases be different from the purely mathematical treatment, however, we believe that the least-squares method

suppresses the random variations thus giving more reliable results. There may arise a question of reliability of the exact periodicity which is inherent to the analysis by a Fourier series. But it seems to us that a joint analysis over more than one year would introduce more inaccuracy into the results.

The selected runs are summarized in Tab. 1, where

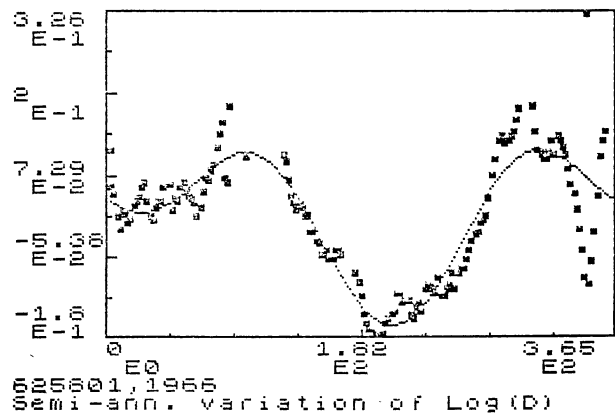


Fig. 1. Observed values of  $\log(D)$  and fitted curve for the satellite 1962 58 A, during 1966,  $h = 208$  km.

the amplitudes and phases for the individual runs are quoted. Several runs were omitted, mostly on the grounds of insufficient number and/or distribution of data during a complete year. Finally, there re-

mained 27 runs during 1966 and 1976 based on the data derived from the orbits of 9 satellites.

After the statistical analysis of all those individual results we found a formula for the annual and semi-annual variation of the density,

$$(3) \quad \Delta \log \varrho_A = (-0.0272 + 2.639 \times 10^{-4}h) \cdot \cos [\Omega'(d - 9.759)] + (0.0285 + 1.819 \times 10^{-4}h) \cdot \cos [2\Omega'(d + 75.71 - 0.0043h)],$$

where  $\Omega' = 2\pi/365$ , heights  $h$  being in km.

Comparing this formula to Eq. (3) in Sehnal et al. (1986), we see that there is no quadratic term in the second amplitude  $C_2$  but the other height dependences are found to be in relatively good agreement. There are similar linear changes of the first amplitude and of the second phase. From our point of view the quadratic term of the second amplitude in Sehnal et al. (1986) is not real but possibly caused by the inadequate accuracy of the original data.

Since there was a misprint (constant term of the second amplitude  $C_2$ ) in formula (3) of Sehnal et al. (1986), we repeat the proper form of the equation here again:

$$(4) \quad \Delta \log \varrho_A = (0.01004 + 1.375 \times 10^{-4}h) \cdot \cos [\Omega'(d + 30.94)] + (-0.03208 + 1.4428 \times 10^{-4}h + 7.714 \times 10^{-7}h^2) \cdot \cos [2\Omega'(d + 101.45 - 0.0972h)].$$

We now compare the curves given by Eqs. (3) and (4) to that used in the CIRA 72 model. In the formula used by Oliver (1980), the annual change is given by the expression

$$(5) \quad \Delta \log \varrho_A = f(h) g(\tau), \\ f(h) = 5.876 \times 10^{-7} h^{2.331} + 0.06328 \exp(-2.868 \times 10^{-3}h), \\ g(\tau) = 0.02835 + 0.3817[1 + 0.4671 \sin(2\pi\tau + 4.137)] \cdot \sin(4\pi\tau + 4.259), \\ \tau = \Phi + 0.0954, \\ \cdot [\{\frac{1}{2} + \frac{1}{2} \sin(2\pi\Phi + 6.04)\}^{1.65} - \frac{1}{2}], \\ \Phi = (t - t_0)/T,$$

where  $t_0 = \text{Jan. } 1.0$ , and  $T$  is the tropical year in days,  $t$  being the day count in a year.

Since formula (4) is actually valid in the range

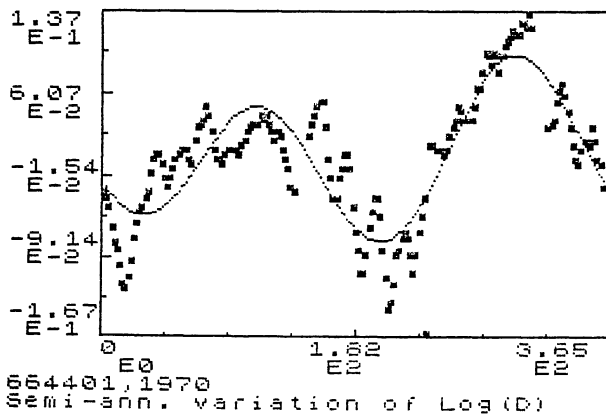


Fig. 2. Observed values of  $\log(D)$  and fitted curve for the satellite 1966 44 A, during 1966,  $h = 297$  km.

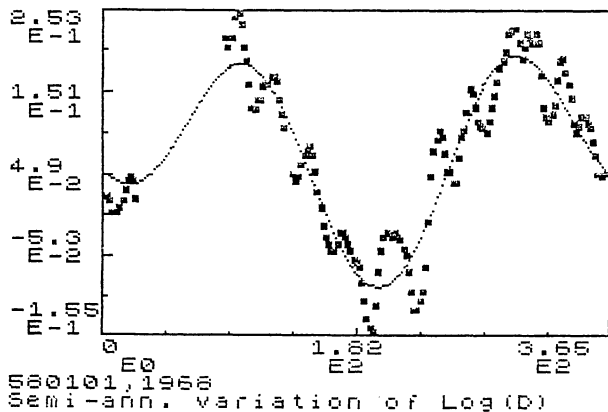


Fig. 3. Observed values of  $\log(D)$  and fitted curve for the satellite 1958 01 A, during 1966,  $h = 331$  km.

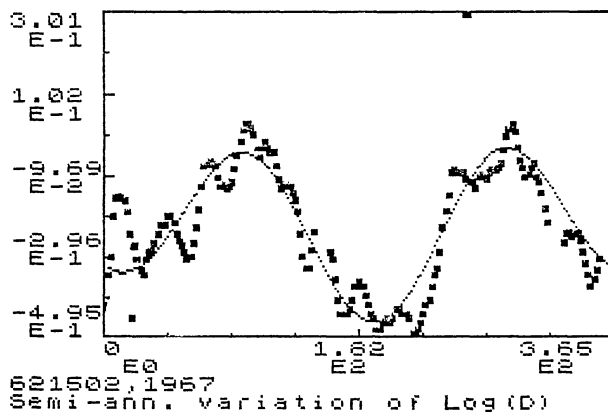


Fig. 4. Observed values of  $\log(D)$  and fitted curve for the satellite 1962 15 B, during 1967,  $h = 393$  km.

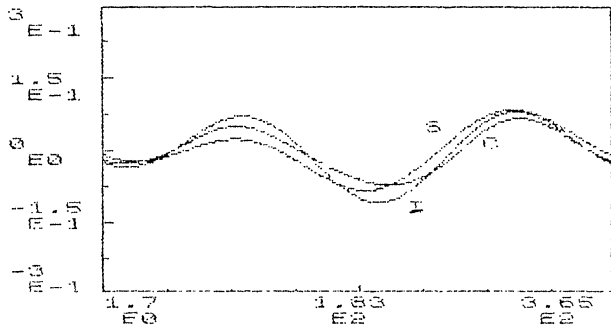


Fig. 5. Comparison of the semi-annual variation of  $\log(D)$  at the height of 250 km (C — CIRA 72, S — Sehna et al. 1986, I — Eq. (3) of this paper).

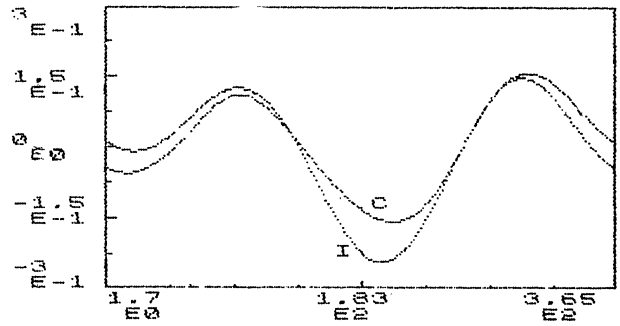


Fig. 9. Comparison of the semi-annual variation of  $\log(D)$  at the height of 560 km (C — CIRA 72, I — Eq. (3) of this paper).

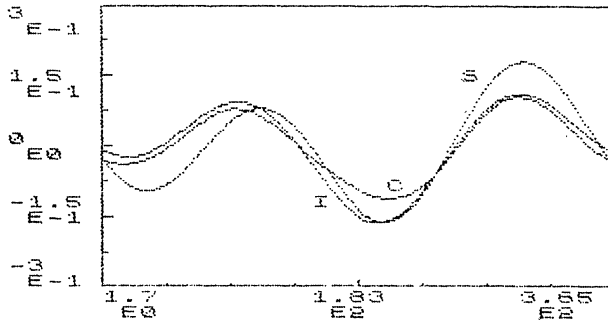


Fig. 6. Comparison of the semi-annual variation of  $\log(D)$  at the height of 375 km (C — CIRA 72, S — Sehna et al. 1986, I — Eq. (3) of this paper).

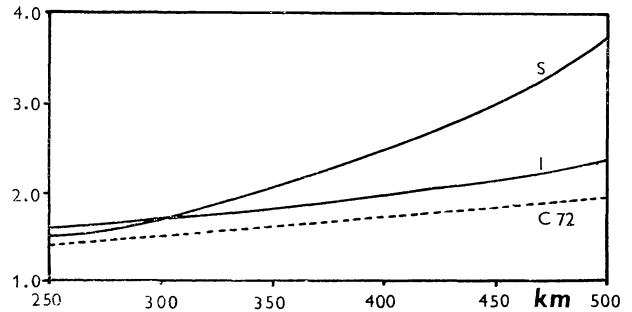


Fig. 10. The growth with height of the amplitude (autumn max. vs. summer min.) of the semi-annual density variation (C — CIRA 72, S — Sehna et al. 1986, I — Eq. (3) of this paper).

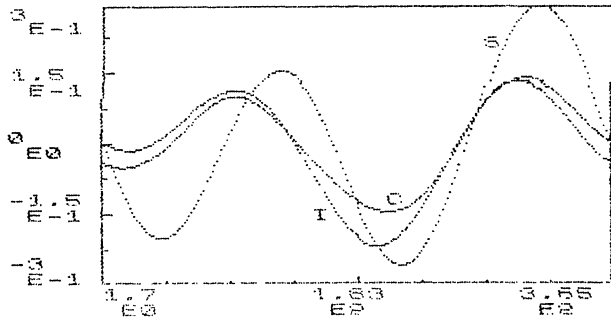


Fig. 7. Comparison of the semi-annual variation of  $\log(D)$  at the height of 500 km (C — CIRA 72, S — Sehna et al. 1986, I — Eq. (3) of this paper).

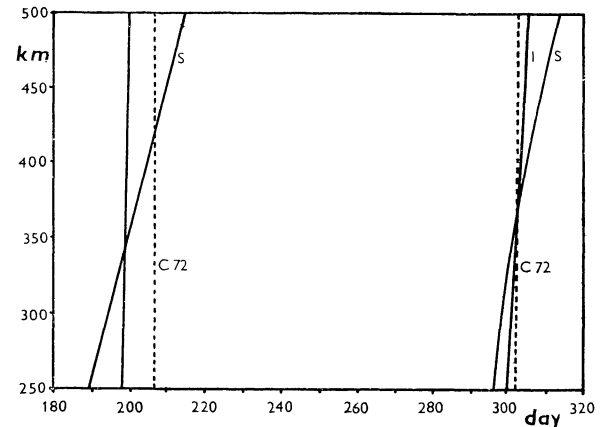


Fig. 11. The shift of the principal minimum (around  $d = 200$ ) and of the principal maximum (around  $d = 300$ ) with growing height (C — CIRA 72, S — Sehna et al. 1986, I — Eq. (3) of this paper).

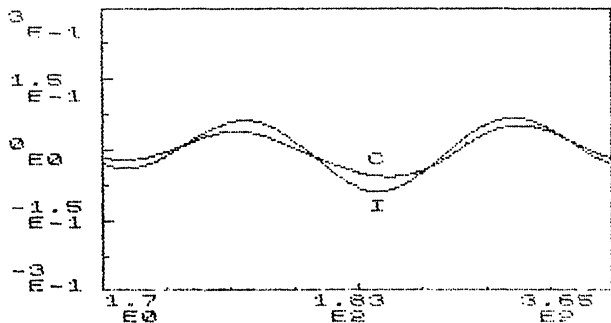


Fig. 8. Comparison of the semi-annual variation of  $\log(D)$  at the height of 200 km (C — CIRA 72, I — Eq. (3) of this paper).

of 250 to 500 km only, we have in Figs. 5 to 7 the comparison of the semi-annual variation as given by Eqs. (3), (4) and (5) for heights of 250, 375 and 500 km. Figures 8 and 9 then show the comparison of formulas (3) and (5) for the heights of 200 and 560 km which are out of validity of formula (4) by definition (Sehna et al. 1986).

## 5. Conclusion

Looking at Figs. 5 to 9, it is easy to recognize that there is no substantial difference between the curves at 250 km. Perhaps the "S" and "I" curves indicate a somewhat deeper principal minimum than that of CIRA 72 (curve "C"). The same is true for higher altitudes, so that we can claim that  $Q_{\min}$  of CIRA 72 in June–July is somewhat higher than it should be. This effect can be seen in Figs. 8 and 9 as well; the overestimation increases with height. On the other hand, the autumn maximum becomes more and more underestimated with increasing height. This means that the amplitude given by CIRA 72 is smaller than that derived from observations. It is demonstrated in Fig. 10, where the observed

amplitude increases with height more than the corresponding CIRA 72 values. The positions of the extreme values during the year are given in Fig. 11. There is no phase shift with height in CIRA 72, however, both the "S" and "T" curves derived from observations show a shift with height.

## REFERENCES

- Horváth A., Illés-Almár E. 1970 *Nabl. Isk. Sputnikov Zemli* 9, 277  
 King-Hele D. G. 1964 *Theory of Satellite Orbits in an Atmosphere*, Butterworths, London  
 Oliver W. L. 1980 *Lincoln Laboratory Tech. Note No. 1980-20*  
 Sehnal L., Helali Y. E., Tawadrous M. Y., Baghos B. B. 1986 *Bull. Astron. Inst. Czechosl.* 37, 196  
 Walker D. M. C. 1977 *Space Res.* XVIII, 291

## SHADOW FUNCTION – CONTRIBUTION TO THE THEORY OF THE MOTION OF ARTIFICIAL SATELLITES

Josef Kabeláč

*Department of Geodesy, Czech Technical University, Thákurova 7, 166 29 Praha 6, Czechoslovakia*

Received 4 June 1987

### ФУНКЦИЯ ТЕНИ – ВКЛАД В ТЕОРИЮ ДВИЖЕНИЯ ИСКУССТВЕННЫХ СПУТНИКОВ

Дается уточненная теория функции тени. Учитываются следующие геометрические факторы: — взаимное положение Солнца, Земли и спутника, — форма конических поверхностей тени, — влияние рефракции. Кроме того приняты во внимание следующие физические влияния: — диффузия света вследствие рефракции, — атмосферное поглощение, — диффузия света, и — влияние озона. Полученная функция тени сравнивается с фотометрическими наблюдениями захода Солнца со спутника. Доказано, что одной геометрии тени не достаточно. Влияние выведенной функции тени по сравнению с более ранними проявится в элементах орбит как 0,1%—1% полного значения от давления солнечного излучения. В заключение обсуждаются некоторые дальнейшие перспективы.

A more precise version of the theory of the shadow function is presented. Considered are the following geometrical factors: — the mutual position of Sun, Earth and satellite, — the shape of the conical surface shadows and — the effect of refraction. Further the following physical effects are taken into account: — light diffusion due to refraction, — atmospheric absorption, — light diffusion and — the effect of ozone. The resulting shadow function is compared to photometric measurements of the sunset, as observed from the satellite. It has been shown that the geometry alone of the shadow is not sufficient enough. The influence of the shadow function introduced in the present paper compared to the shadow functions, given earlier, displays differences in the orbital elements amounting to 0.1% to 1% of the total value of the solar radiation pressure. Some further perspectives have been accounted for in the conclusion.

**Key words:** artificial satellites: perturbations, shadow function